Journal of Biosensors & Bioelectronics
ISSN: 2155-6210

Arora et al., J Biosens Bioelectron 2017, 8:3
DOI: 10.4172/2155-6210.1000246

Research Article OMICS International

Modified Tin Oxide Based Bioelectrode for Reagentless Detection of Uric Acid

Kashima Arora[1], Monika Tomar[2] and Vinay Gupta[1]*

[1]Department of Physics and Astrophysics, University of Delhi, Delhi, India
[2]Department of Physics, Miranda House, University of Delhi, Delhi, India

Abstract

A reagentless uric acid biosensor has been realized using Copper implanted tin oxide thin film (Cu:SnO_2) based matrix. The biosensing characteristics of implanted matrix have been studied using the electrochemical impedance spectroscopy and cyclic voltammetry. The prepared matrix (Cu:SnO_2), because of the presence of Cu, possess redox properties so that the electron transfer from enzyme to the electrode could be accomplished without using any external mediator in the electrolyte. The developed uric acid biosensor exhibits a high sensitivity of about 0.93 mA/mM and a linear variation in current response over a concentration range from 0.05 to 1.0 mM of uric acid besides high shelf life (~20 weeks). The Michaelis-Menten kinetic parameter (K_m) is found to be relatively very low (0.12 mM), which indicates the high affinity of the fabricated bioelectrode towards the uric acid (analyte). The results highlight the importance of implanted Cu:SnO_2 thin film as an attractive matrix for the realization of reagentless biosensors towards uric acid.

Keywords: Reagentless uric acid biosensor; RF sputtering; Cu implanted SnO_2

Introduction

Uric acid is present in number of biological fluids including urine and blood serum and is associated with the presence of diseases such as gout, hyperuricemia, cholesterol, arthritis, renal, neurological, kidney diseases etc. Thus, efficient detection of uric acid in human blood is of great interest to the researchers. Many reports are available on the detection of uric acid [1,2], but the presence of external mediator in the electrolyte hinders its usage for implantable biosensor. Limited work has been carried out on the development of reagentless uric acid biosensors, where no external mediating element is needed. Table 1 summarizes the work carried out on uric acid biosensors by various workers using different matrices. Various matrices have been utilized for the detection of uric acid such as APTES Bis sulfosuccinimide/ITO [3], gold electrode/polystyrene [4], carbon felt based H_2O_2 [5], poly N-isopropyl acrylamide MWCNT-Ch/poly(amidoamine)/DNA/gold electrode [6], Polyaniline [7], screen printed electrode [8] and so on. However, the low sensitivity and poor shelf life of the biosensors are major concern. Metal oxide thin film-based bioelectrodes are shown to be advantageous. Tin oxide (SnO_2), a wide band gap semiconductor (E_g=3.87 eV), has multifunctional properties for broad range of applications including transparent electronics, gas sensors, acoustic devices, UV photo detectors, etc.

Recently SnO_2 is being explored for biosensing applications owing to its excellent charge transfer capability, good biocompatibility, low cost, abundance in nature etc. [9]. However, the non-redox property of SnO_2 demands an external mediator in the electrolyte, which hinders its application for realizing an integrated biosensor. Few attempts have been made towards tailoring the properties of metal oxides by introducing suitable metal dopants [10]. The metal ions having multiple valence states such as Fe, Cu, Mn, V etc. can be incorporated to induce redox properties in the host metal oxide matrix [11]. However, most of the reports on doped metal oxide matrix are using chemical route which lead to the preparation of bioelectrodes with poor stability [12]. The rapid decay in the response of these bioelectrodes with time may be due to poor incorporation of metal dopants at the lattice sites of host oxide matrix and poor quality of deposited films. Implantation is an effective method to incorporate the foreign elements in the metal oxides and to tailor its properties. Few reports are available on incorporating redox species into the ZnO matrix using ion implantation of Fe for reagentless detection of glucose [13]. Surprisingly, no efforts are being made to modify the electronic properties of SnO_2 by implanting it with suitable metals that have multiple oxidation states especially for detection of uric acid. Amongst different metals, copper (Cu) has multi-electron oxidation states and is attractive due to natural abundance, low cost, non-toxic and good electrochemical activity [6,14]. The impantation of Cu in SnO_2 may induce the redox property besides enhancing the electron transfer property for possible biosensing application.

In this paper, the SnO_2 thin films were prepared by RF sputtering technique and Cu implanted SnO_2 matrix has been utilized for development of reagentless uric acid biosensor. The biosensor is found to be exhibiting excellent response characteristics important for use in implantable biosensor chip.

Materials and Methods

Materials

Uric acid (99.99% pure), Uricase (1 mg/mL) horseradish peroxidase (HRP) and o-dianisidine dye were procured from Sigma-Aldrich. Sodium phosphate monobasic anhydrous and sodium phosphate dibasic dihydrate (analytical reagent grade) were obtained from Sisco Chemical, India. All the chemicals were used without any further purification. Deionized water having a high resistivity of 18.2

***Corresponding author:** Vinay Gupta, Department of Physics and Astrophysics, University of Delhi, Delhi 110007, India, Tel: 011 2700 6900; E-mail: vgupta@physics.du.ac.in

Received August 10, 2017; **Accepted** August 23, 2017; **Published** August 30, 2017

Citation: Arora K, Tomar M, Gupta V (2017) Modified Tin Oxide Based Bioelectrode for Reagentless Detection of Uric Acid. J Biosens Bioelectron 8: 246. doi: 10.4172/2155-6210.1000246

S.No.	Material	Range	Sensitivity	Response time	Km	Detection limit	Ref.
1.	SAM of APTES Bis sulfosuccinimide/ITO	0.05-0.58 mM	39.35 μA_{mM}-1	50 s	-	0.037 mM	3
2.	Gold electrode/polystyr ene	5-105 µM		Within 1 min	-		4
3.	ZnO nanowires	1-1000 µM	32 mV/decade	9s	-	1 µM	20
4.	Carbon felt based H_2O_2	0.3-20 µM	0.25 µA mM^{-1}		-	0.18 µM	5
5.	MWCNT- Ch/poly (amidoa mine)/DNA/ gold electrode	0.5-100 µM	43.9 nA/mM	5s	-	0.07 µM	6
6.	Polyaniline	0.01-0.6 mM	47.2 mA/mM	60s	5.1 × 10^{-3} mM/L	0.01 mM	7
7.	Polyurethane hydrogel	0 -2 mM		80-100s			21
8.	Screen printed electrode	2-40µM	3.05 µA μM^{-1}			0.42 µM	8
9.	Poly(o- aminophenol) C paste electrode	Upto 10^{-4} M	5µA	37s		3X10^{-6} M	22
10.	MWCNT/Au nps.	0.01-0. 8 mM	0.44 mA mM^{-1}	7 s	0.5 mM	0.01 mM	23
11.	3 amino5- mercapto-124 triazole/GC	40 nM-0.1 mM		50 s		0.52 nM	24
12.	Epoxy resin biocomposite	0.025-0.1 mM		12 s	0.17 mM	4.25 µg/mL	25
13.	Ir-C electrode	0.1-0.8 mM	16.60 µM/mM	<45 s		0.01 mM	26
14.		0.005-0.8 mM		4s	0.058 mM	5 µM	27
15.	Mercaptoethylpy razine/Au	5-150 µM	3.4 ± 0.08 $nA_{cm^{-2}\ \mu M^{-1}}$	80-100s	290 µM	2µM	28

Table 1: Brief summary of the important reports on uric acid biosensors.

MΩ cm was used for the preparation of aqueous solutions. Different concentrations of uric acid solution (0.05-1.0 mM) and solution of o-dianisidine (1%) dye were freshly prepared in de-ionized water.

Cu implanted SnO_2 thin film based electrode

A 100 nm thin Pt layer was deposited on the surface of corning glass slide over an area of 2 cm × 1 cm by RF sputtering technique using a 3 inch diameter metal Pt target (99.99% pure) under 100% Ar gas ambient and a power of 100 W. A buffer layer (~ 10 nm) of titanium (Ti) was sputter coated prior to Pt deposition under the same growth condition onto the glass slide using a Ti target (99.99% pure) to improve the adhesion of Pt on the glass slide. SnO_2 thin film was deposited on to Pt/Ti coated Corning glass slide using RF magnetron sputtering technique on an area of 1cm×1cm while the remaining 1 cm × 1 cm area was protected using shadow mask for electrical connections. A 2 inch diameter metallic tin target (99.999% pure) was sputtered in a reactive gas mixture (70% Ar and 30% O_2) at an rf power of 30 W and sputtering pressure of 20 mTorr. The thickness of SnO_2 thin film was maintained at 180 nm. Subsequently, Copper (Cu) was implanted in as-grown SnO_2 thin film at room temperature at low energy (15 keV) to a fluence of 10^{15} and 10^{16} cm^{-2}. The ion implantation was carried out on low energy ion implanter -150 kV accelerator at the Australian National University, Australia. The biosensor electrode for detection of uric acid has been prepared on Cu implanted SnO_2 matrix and the fabrication steps are shown schematically in Figure 1.

Preparation of PBS solution: Phosphate Buffer Saline (PBS) solution (50 mM) of pH 7 was prepared by adjusting the proportion of monobasic sodium phosphate solution and dibasic sodium phosphate solution and then adding 0.9% NaCl to the solution. PBS containing $[Fe(CN)_6]^{3-/4-}$ solution was prepared by adding 5mM potassium ferrocyanide $[K_4Fe(CN)_6]$ and potassium ferricyanide $[K_3Fe(CN)_6]$ in the prepared PBS solution for electrochemical impedance spectroscopy (EIS) measurements. Cyclic voltammetry (CV) measurements were carried out in PBS solution without the addition of any external mediator such as ferro/ferri cyanide.

Preparation of Bioelectrode: Immobilization of Uricase on Cu implanted SnO_2 matrix: The fabrication process of bioelectrode (Uricase/Cu:SnO_2/Pt/glass) is schematically shown in Figure 1. In order to prepare the bioelectrode, Cu implanted SnO_2 matrix was hydrolysed by immersing the electrode (Cu:SnO_2/Pt/Ti/glass) in a solution of H_2O_2/ NH_4OH/ H_2O (1:1:5, v/v) for 30 min at 80 ^{0}C. The hydrolyzed matrix was immersed in 1% (v/v) solution of APTES in toluene overnight at room temperature for silanization. After the coupling reaction, the electrodes were rinsed with toluene and water to remove the loosely bound silanes from the surface of implanted matrix. The modified electrodes after silanization were dried under a stream of nitrogen. Uricase was covalently attached to the functionalized electrodes using EDC/NHS chemistry. The amount of enzyme used for immobilization was optimized and maximum binding was observed when 5 µl of uricase solution was diluted to 30 µl in distilled water containing 0.4 M EDC and 0.1 M NHS. The enzyme solution was poured onto 1 cm^2 area of the electrode having functionalized Cu:SnO_2 matrix and kept for approximately 4 h in a humid chamber at room temperature for the binding of uricase using cross linkers. The bioelectrode was dried under nitrogen flow and stored at 4 °C when not in use.

Characterization techniques

The structural and optical properties of the developed Cu implanted SnO_2 matrix were studied using an X-ray diffractometer (Bruker D8 Discover) and a double beam Uv-visible spectrophotometer (Perkin Elmer, Lambda 25-35-45) respectively. Implantation of Cu into SnO_2 matrix is confirmed by energy-dispersive X-ray spectroscopy (EDX) analysis. Modification of surface morphology before and after immobilization of the uricase were investigated using an atomic force microscope (Veeco DICP2) in non-contact mode, a scanning electron microscope and a fourier transform infrared spectrophotometer (Perkin Elmer (Model Spectrum BX). Micro images obtained from AFM were analyzed by SPM Lab Analysis software. Electrochemical measurements were carried out on a potentiostat/galvanostat/ZRA (Gamry reference using a conventional three-electrode electrochemical cell with Ag/AgCl as reference electrode, platinum (Pt) foil as counter electrode and uricase/Cu:SnO_2/Pt/Ti/glass as working electrode. The enzyme activity of bio-electrode was studied using UV–visible spectrophotometer (Perkin Elmer, Lambda 35). The thickness of deposited thin film was determined using surface profiler (Dektak 150A). PBS solution (10 ml, 50 mM, 0.9% NaCl) without any mediating species was used as electrolyte.

Results and Discussion

X-Ray Diffraction (XRD) studies

The XRD studies of as-deposited SnO_2 films shows the growth of amorphous film, which became polycrystalline after a post deposition

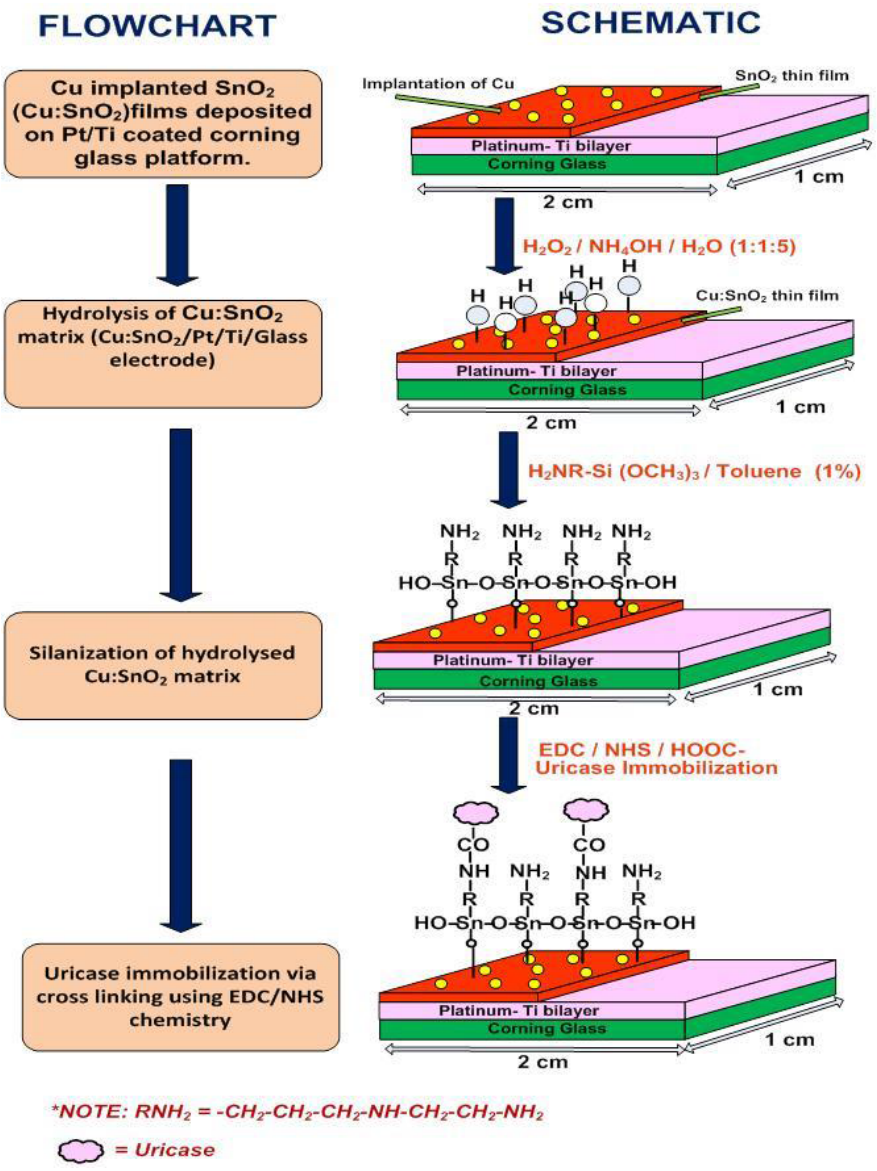

Figure 1: Schematic of Immobilization of uricase on Cu implanted SnO_2 matrix via EDC/NHS chemistry.

annealing treatment at 300°C in air for 2 h. The XRD spectrum for the annealed SnO_2 film deposited on glass slide is shown in Supplementary Figure 1a. Well defined reflection peaks corresponding to (110), (101), (200) and (211) planes of rutile SnO_2 were observed in the XRD pattern [15], indicating that the annealed SnO_2 thin film is polycrystalline. The average crystallite size of the SnO_2 film was calculated from the dominant (101) XRD peak using the Debye Scherrer's formula and is found to be about 9 nm.

XRD patterns of the Cu implanted SnO_2 films are shown in Supplementary Figure 1b and 1c. It may be seen from Figure 2 that no peak corresponding to Cu was observed in the XRD pattern of Cu implanted SnO_2 thin films. However, SnO_2 film became preferred oriented along (101) direction with implantation of Cu (Supplementary Figure 1). The crystallinity of SnO_2 thin film improves with increasing the fluence of Cu implantation. The observed improvement may be associated with the recrystalization of the SnO_2 film surface on ion implantation and substitution of Cu ions at its lattice sites (Supplementary Figure 1). The crystallite size of implanted samples is found to be almost same (10 nm) as that of pure SnO_2 film.

Energy-dispersive X-ray spectroscopy (EDX) analysis of Cu implanted SnO_2 matrix

EDX spectra of bare SnO_2 and Cu implanted (10^{16} cm^{-2} fluence) SnO_2 films deposited on Pt coated Si wafer are shown in Figure 2. The presence of both Sn and O can be easily seen in the EDX spectra along with the weak peaks corresponding to Pt and Si, which are due to the underneath Pt electrode and Si wafer, respectively. The additional peaks observed corresponding to the Cu in the EDX spectra of Cu implanted SnO_2 film (Cu:SnO_2), clearly confirm the presence of Cu in the implanted SnO_2 matrix.

Electrochemical studies of electrodes

Cyclic voltammetry: The cyclic voltammograms (CVs) of SnO_2/Pt/glass and Cu:SnO_2/Pt/glass electrodes were recorded in the PBS

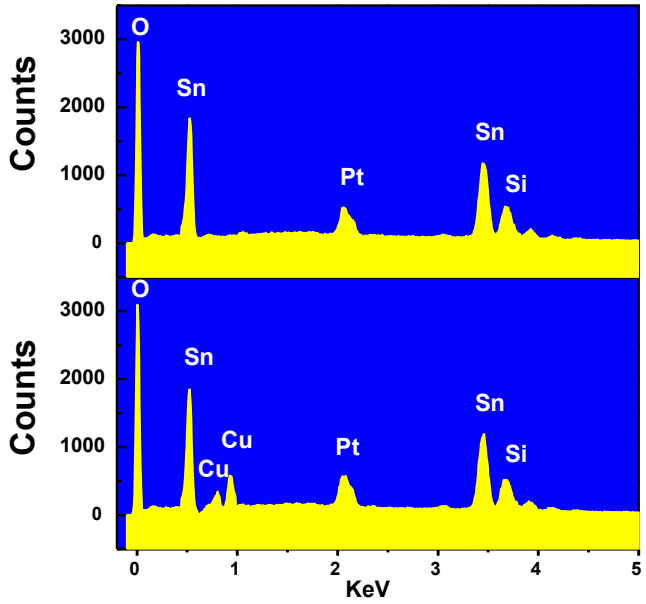

Figure 2: EDX spectra of the (a) bare SnO_2 film and (b) Cu implanted SnO_2 film at a fluence of 10^{16} cm^{-2}.

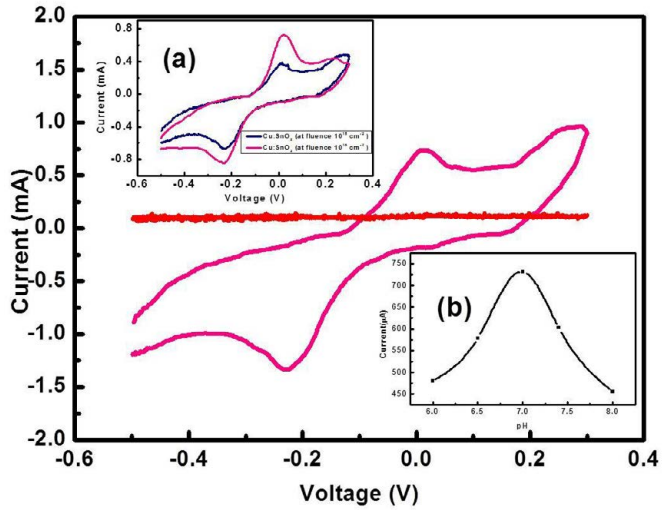

Figure 3: Cyclic voltammograms of SnO_2/Pt/glass and Cu:SnO_2/Pt/glass electrodes in PBS buffer. Insets (a) and (b) shows the Cyclic voltammograms of Cu implanted SnO_2 at fluences of 10^{15} and 10^{16} cm^{-2} and variation of peak oxidation current (I_{pa}) with pH for the bioelectrode implanted with 10^{16} Cu/cm^{-2}, respectively.

electrolyte without any redox speciclearly seen that no redox peak is observed in the CV spectra for SnO_2/Pt/Ti/glass electrode in PBS solution in the entire measured range of voltage (-0.5 V–0.3 V) because SnO_2 does not have any redox couple of its own. Hence, in the absence of any mediator in the electrolyte solution SnO_2 does not show any redox peak. On the other hand, the CV spectrum of Cu:SnO_2/Pt/glass electrode, clearly shows well defined redox peaks in a mediator-free PBS buffer which is attributed to valence transformation of copper from Cu^{1+} to Cu^{2+} and vice-versa, thus resulting in accelerated electron transfer. These results indicate that Cu is responsible for the reversible redox property in the electrode and serves as the electron transfer channel. The value of peak oxidation current obtained for Cu implanted SnO_2/Pt/Ti/glass matrix was found to be much higher in comparison to that reported for other ion implanted metal oxide matrices for biosensing such as Fe:ZnO [16]. It may be clearly seen from inset (a) of Figure 3 that the electrode implanted at a fluence of 10^{16} cm^{-2} gives higher peak oxidation current (0.72 mA) than at lower fluence and hence chosen for further studies.

Immobilization of enzyme onto the Cu:SnO_2/Pt/Ti/glass electrode

Atomic force microscopy: The AFM images showing surface morphology of the Cu implanted SnO_2 (fluence 10^{16} cm^{-1}) before and after immobilization of uricase is shown in Figure 4a and 4b, respectively. The surface morphology of the Cu implanted SnO_2 thin

film was rough (average roughness ~10 nm) with fine microstructure having uniformly distributed small size grains, and is beneficial for the efficient loading of enzyme on its surface. Upon immobilization of uricase on the surface of implanted matrix, clusters of uricase bio-molecules forming a globular structure of much bigger size (~ 2 μm) are seen Figure 4b. This confirms the successful immobilization of enzyme (uricase) onto the surface of Cu:SnO_2/Pt/Ti/glass electrode.

FTIR studies

The prepared Cu implanted SnO_2 films were characterized by FTIR spectroscopy before and after immobilization of enzyme and the corresponding spectra are shown in Supplementary Figures 2a and 2b, respectively. The sharp and well defined absorption peak observed at around 606 cm^{-1} in Supplementary Figure 2a corresponds to the SnO_2 lattice mode [17]. The absorption bands observed at around 2852, 1359 and 1094 cm^{-1} (Supplementary Figure 2a) can be assigned to the –OH groups attached directly to the surface oxygen of the SnO_2 film [18]. The absorption band at 1660 cm^{-1} is attributed to H–O–H in-plane deformation. The interaction of the O–OH–group can be seen at 2047 and 2452 cm^{-1}. The absorption band observed at 508 cm^{-1} corresponds to the vibrations related to Cu, which confirms that the Cu is efficiently implanted into the SnO_2 thin film matrix. Binding of the enzyme (uricase) onto the surface of Cu:SnO_2/Pt/Ti/glass electrode is revealed by the appearance of additional absorption bands at around 1071, 1175, 1640, 2157, 2922 and 3370 cm^{-1} (Supplementary Figure 2b). The sharp band at 1640 cm^{-1} (Supplementary Figure 2b) is associated with the carbonyl stretch (amide 1 band). The band at 1071 and 1175 cm^{-1} correspond to C-H bonding of alkene and C-N vibrations, respectively. The bands at 2157 and 2922 cm^{-1} corresponds to –CH stretching of $–CH_2$ groups. Furthermore, a broad absorption peak at 3370 cm^{-1} (Supplementary Figure 2b) is related to the O-H stretching mode. The presence of observed stretching modes confirm the effective immobilization of uricase onto the surface of Cu:SnO_2 thin film matrix.

Electrochemical impedance spectroscopy (EIS)

Electrochemical impedance spectroscopy (EIS) analysis has been carried out using a three-electrode cell with the SnO_2/Pt/Ti/glass and Cu:SnO_2/Pt/T/glass electrodes as working electrode, platinum (Pt) foil as counter electrode and Ag/AgCl as reference electrode in PBS solution containing $[K_3Fe(CN)_6]^{3-/4-}$ as the mediator in the frequency range 100 kHz to 10 mHz. Supplementary Figure 3 shows the Nyquist plots obtained for (i) SnO_2/Pt/Ti/glass electrode, (ii) Cu:SnO_2/Pt/Ti/glass electrode and (iii) Uricase/ Cu:SnO_2/Pt/Ti/glass bioelectrode. The Nyquist plot includes a semicircle portion corresponding to the electron-transfer-limiting process and a linear part resulting from the diffusion-limiting step of the electrochemical process (Supplementary Figure 3). The diameter of the semicircle gives the electron-transfer resistance (R_{ct}) of the electrode–solution interface. The values of charge transfer resistance (R_{ct}) obtained from Supplementary Figure 3 for SnO_2/Pt/Ti/glass, (ii) Cu:SnO_2/Pt/Ti/glass and (iii) Uricase/ Cu:SnO_2/Pt/Ti/glass electrodes are found to be about 460 ohms, 250 ohms and 350 ohms, respectively. The value of R_{ct} shows the electron-transfer kinetics of the redox probe at the electrode interface. Thus, the observed decrease in the value of R_{ct} of the electrodes from 460 ohms to 250 ohms, after implantation of Cu into SnO_2 matrix (Supplementary Figure 3, curve (ii)), indicates the improved charge transfer characteristics of the implanted Cu:SnO_2 matrix. This is due to metallic character of the incorporated Cu into SnO_2 matrix which provides electron conduction channel between the electrode and electrolyte. The enhancement in the R_{ct} value to 350 ohms for uricase/Cu:SnO_2/Pt/Ti/glass bioelectrode, Supplementary Figure 3, curve (iii) confirms the binding of bulky non-conducting macromolecules of enzyme onto the surface of Cu:SnO_2 matrix which provide hindrance to the conduction of charge carriers..

Sensing response characteristics

It is known that the pH of the electrolyte solution changes the activity of the biomolecules to a great extent. CV response of the prepared uricase/Cu:SnO_2/Pt/Ti/glass bio-electrode was investigated at various pH levels (6.0 to 8.0) of the PBS buffer and the variation of the peak oxidation current (I_{pa}) with pH is shown in the inset of Figure 3. The peak oxidation current (I_{pa}) was found to increase with an increase in pH from 6.0 to 7.0 having a maximum value of 750 μA and decreases thereafter with further increase in pH. Therefore, the pH of the PBS solution was kept at 7.0 for amperrometric studies. The CV spectra were recorded for uricase/Cu:SnO_2/Pt/Ti/glass bioelectrode at varying scan rates from 100 to 600 mV/s as shown in Supplementary Figure 4. Both the oxidation (I_{pa}) and reduction (I_{pc}) peak currents were found to increase linearly with the increase in scan rate from 100 to 600 mV/s (inset of Supplementary Figure 4). The linear relationship between the peak currents (I_{pa} or I_{pc}) and scan rate (ν) demonstrates that the electrochemical reaction of immobilized uricase on Cu implanted SnO_2 electrode is a surface-controlled process. Furthermore, the redox potentials corresponding to the anodic and cathodic peak currents shift respectively towards the higher potential and lower potential with

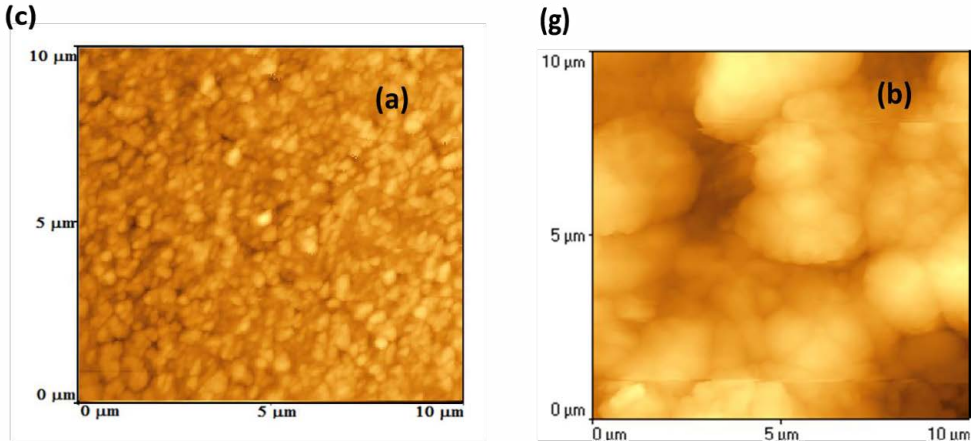

Figure 4: AFM image of the surface of Cu implanted SnO_2 electrode at a fluence of 10^{16} cm^{-2} (a) before and (b) after uricase immobilization.

increase in scan rate (Supplementary Figure 4). The observed variation in redox potential confirms that the reaction is quasi-reversible.

The surface concentration of ionic species per unit area for uricase/Cu implanted SnO_2/Pt/Ti/glass bio-electrode is estimated using Brown-Anson model. The estimated value of surface concentration of electroactive uricase on the surface of the prepared bioelectrode is found to be about 5.42×10^{-5} mole/cm^2 which is greater in comparison to the corresponding values reported by various workers for uric acid biosensors using other metal oxide matrices [5,6]. The high surface concentration obtained in the present work confirms that the prepared bioelectrode offers high enzyme loading. This is attributed to the preparation of implanted matrix with desired rough surface morphology. The high enzyme loading is expected to provide the enhanced sensitivity of the developed biosensor. The results indicate that Cu implantation is effective not only in enhancing the electron communication property of SnO_2 matrix, but also in increasing the electroactive surface area of the matrix.

The sensing response of the bioelectrode (uricase/Cu:SnO_2/Pt/Ti/glass) has been obtained using the CV spectra recorded with increasing concentration of uric acid in the PBS electrolyte (Figure 5). The physiological range of uric acid in human serum is between 0.13 to 0.46 mM. Thus, the concentration of uric acid (analyte) was varied from 0.05 to 1.0 mM in the electrolyte solution. It may be observed from Supplementary Figure 5 that the oxidation peak current increases linearly from 0.17 mA to 1.09 mA with an increase in uric acid concentration from 0.05 to 1.0 mM. The CV responses were used to draw a calibration curve for the uricase/Cu:SnO_2/Pt/Ti/glass electrode on interaction with the varying concentration of uric acid as shown in the inset (a) of Figure 5. It may be clearly seen from the calibration curve that the uricase/Cu:SnO_2/Pt/glass electrode exhibits good linearity for the sensing of uric acid in a wide range from 0.05 mM to 1.00 mM with a correlation coefficient of 0.99. Sensitivity of the uricase/Cu:SnO_2/Pt/glass bioelectrode is calculated from the slope of the calibration curve and is found to be about 0.93 mA/mM with a low limit of detection (LOD) of 0.06 mM. Sensitivity of the bioelectrode towards uric acid is found to be higher compared to the corresponding values reported by various workers for other metal oxide matrices (Table 1). Furthermore, the bioelectrode is found to exhibit fast response time of about 4 seconds due to the fast electron transfer between the active sites of enzyme and electrode. The affinity of uricase immobilized on the surface of the Cu:SnO_2 film towards uric acid is determined from the value of Michaelis–Menten kinetic parameter (K_m) estimated from Hanes plot as shown in the inset (b) of Figure 5. The estimated value of K_m is found to be about 0.12 mM which is lower than values reported by other workers for uric acid biosensors (Table 1). The low value of K_m indicates that the immobilized uricase in the present work has high affinity towards uric acid.

To carry out the photometric enzyme assay, the bioelectrode was dipped in 3 mL PBS solution containing 20 µL horseradish peroxidise (HRP), 20 µL o-dianisidine dye and 100 µL of analyte (uric acid) in varying concentration. The difference between the values of initial absorbance and final absorbance at 500 nm after 2 min incubation of the bioelectrode was recorded and plotted in Supplementary Figure 5 as a function of uric acid concentration. The enzyme activity is found to increase with an increase in the concentration of uric acid upto 0.7 mM and thereafter shows a saturation effect (Supplementary Figure 5). The amount of bound enzyme on the surface of electrode is determined from the apparent enzyme activity $\left(a_{enz}^{app}\right)$ calculated using the equation:

$$\left(a_{enz}^{app}\right)\left(Ucm^{-2}\right) = \frac{AV}{\varepsilon ts} \quad (1)$$

Where A is the difference in absorbance before and after incubation, V is the total volume (=3.17 cm^3), ε is the millimolar extinction coefficient for o-dianisidine (7.5 for o-dianisidine at 500 nm), t is the reaction time (2 mins.), and s is the surface area of the electrode (1.0 × 1.0 cm^2). The value of apparent enzyme activity of the immobilized uricase on the Cu:SnO_2/Pt/Ti/glass electrode is about 5.01×10^{-2} unit/cm^2. This value is much higher than that obtained by other workers indicating that our bioelectrode provides a better platform and hence more units of uricase are actively working per unit electrode surface area [6,19,7].

The selectivity of our bioelectrode is studied by recording the value of peak oxidation current in CV response on addition of

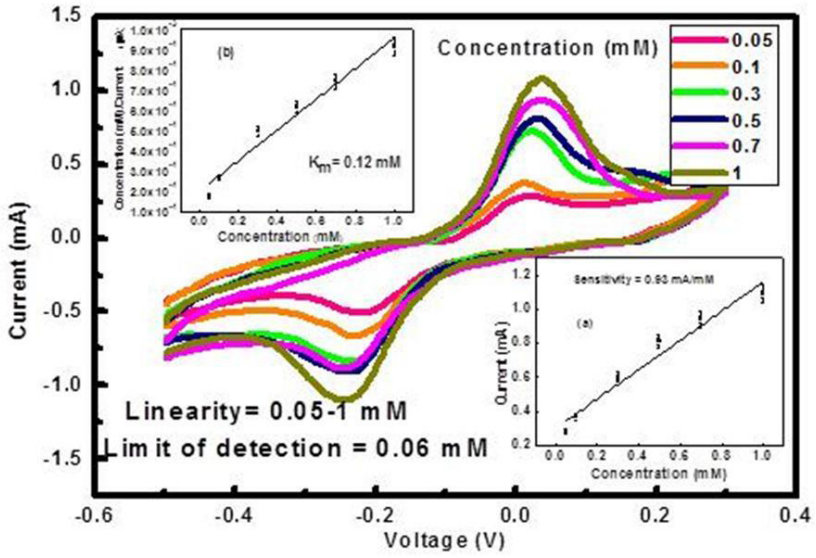

Figure 5: Amperrometric response of uricase/Cu:SnO_2/Pt/Ti/glass bioelectrode as a function of uric acid concentration (0.05 to 1.0 mM). Inset (a) gives the variation in peak oxidation current with uric acid concentration and (b) Hanes plot.

Real Sample (Serum)	Concentration of uric acid measured (mM)		R.S.D. of developed biosensor (n=5) (%)	Spike (mM)	Concentration of uric acid detected (mM)	Recovery (%)	R.S.D. of developed biosensor (n=5) (%)
	Uricase/Cu/SnO_2/Pt/Ti/glass biosensor	Spectrophotometric method					
1	0.312	0.319	1.3	0.5	0.820	101.6	1.2
2	0.235	0.243	1.5	0.5	0.730	99	1.1
3	0.672	0.676	2.1	0.5	1.180	101.6	1.9
4	0.483	0.489	2.5	0.5	0.97	97.4	2.1
5	0.849	0.837	1.8	0.5	1.355	101.2	1.6
6	0.781	0.773	1.2	0.5	1.3	103.8	1.4
7	0.899	0.901	2.9	0.5	1.41	102.2	2.7
8	0.553	0.558	1.3	0.5	1.0	89.4	1.1
9	0.581	0.590	2.3	0.5	1.13	109.8	2.0
10	0.612	0.608	1.6	0.5	1.11	99.6	1.3

Table 2: Determination and recovery of uric acid in human serum samples using the repared uricase/Cu:SnO_2/Pt/Ti/glass biosensor.

normal concentration of various interferents possible in the human serum such as glucose (5.6 mM), cholesterol (5 mM), urea (1 mM), ascorbic acid (0.1 mM) and dopamine (0.1 mM) along with the normal concentration of uric acid (0.3 mM), and the obtained results are shown in inset of Supplementary Figure 5. The insignificant change in value of I_{pa} was observed with all interferents with a maximum interference of 2.1% (inset of Supplementary Figure 5). It may be inferred that the bioelectrode is highly selective towards the uric acid and hence the sensing response is highly reliable. The shelf life studies of the bioelectrode shows that it retains more than 90% of activity even after 20 weeks as shown in Supplementary Figure 6. The enhanced sensing response characteristics are attributed to the preparation of a highly stable and biocompatible Cu implanted SnO_2 thin film matrix in the present study [20-28].

Real samples analysis

The prepared uricase/Cu:SnO_2/Pt/glass biosensor has been exploited for the analysis of uric acid in the real biological fluid, 10 human sera samples were analyzed and the % recovery and precision were calculated for spiked samples. After the addition of the sera samples in the electrolyte solution, the peak oxidation current values have been noted from the CV measurements. Uric acid concentration in serum was then extrapolated from the standard calibration curve between uric acid concentration (mM) and current (inset of Figure 5). Electrochemical sensing technique in the present work has been used to corroborate results obtained by commercial spectrophotometric method in the clinical laboratory. To validate Accuracy of the prepared electrode has been validated by determining the content of uric acid in serum samples and has been compared with that measured by commercial spectrophotometric method in the clinical laboratory. Table 2 summarizes the results obtained during the present investigation. The results indicate that the uric acid analysis in sera with the developed biosensor agrees well with the spectrophotometric data. Recovery tests were also performed in order to demonstrate the accuracy and precision of the prepared biosensor by adding a known concentration of uric acid (0.50 mM) in the already tested serum samples and then estimating the concentration of added uric acid (Table 2). The performed recovery tests confirm that the fabricated biosensor is accurate and precise. The performance of the prepared biosensor system is comparable with the commercially accepted methods. For *in-vivo* application of the biosensor in clinical practice, the requirements of biocompatibility, linearity, sensitivity, specificity, accuracy and long-term stability were very well fulfilled by uricase/Cu:SnO_2/Pt/Ti/glass based biosensor.

Conclusion

A novel reagentless uric acid biosensor based on efficient transfer of electron from the immobilized enzyme onto the electrode via implanted Cu in SnO_2 matrix is developed. The uricase/Cu:SnO_2/Pt/glass bioelectrode exhibits enhanced sensitivity (0.93 mA/mM) with good linearity over a wide detection range (0.05 to1.0 mM) in the absence of any external mediator in the PBS solution. The low K_m value (0.12 mM) obtained for the bioelectrode indicates high affinity of uricase immobilized on the surface of Cu:SnO_2 matrix towards uric acid. The apparent enzyme activity is about 5.01×10^{-2} unit/cm^2. The biosensor exhibits very high stability with a shelf-life of about 20 weeks. The observed results confirmed that Cu implanted SnO_2 matrix is attractive for realization of efficient uric acid biosensor with enhanced sensitivity, good selectivity and high stability.

Acknowledgements

Authors are thankful to Professor C Jagadish and Dr Hoe Tan, Australian National University, Australia for carrying out the implantation of copper for present work. Authors are thankful to Department of Science and Technology (DST), Govt. of India for the financial support to carry out the proposed work. One of the authors (KA) acknowledges CSIR for fellowship.

References

1. Jindal K, Tomar M, Gupta V (2012) CuO thin film based uric acid biosensor with enhanced response characteristics. Biosensors and Bioelectronics 38: 11-18.
2. Tyagi M, Tomar M, Gupta V (2013) NiO Nanoparticle-based Urea Biosensor. Biosensors and Bioelectronics 41: 110-115.
3. Ahuja T, Kumar R, Tanwar VK, Sharma V, Singh N, et al. (2010) An amperometric uricacid biosensor based on Bis[sulfosuccinimidyl] suberate crosslinker/3-aminopropyltriethoxysilane surface modified ITO glass electrode. Thin Solid Films 519: 1128-1134.
4. Wang X, Hagiwara T, Uchiyama S (2007) Immobilization of uricase within polystyrene using polymaleimidostyrene as a stabilizer and its application to uric acid sensor. Analytica Chimica Acta 587: 41-46.
5. Wang Y, Hasebe Y (2012) Uricase-adsorbed carbon-felt reactor coupled with a peroxidase-modified carbon-felt-based H_2O_2 detector for highly sensitive amperometric flow determination of uric acid. Journal of Pharmaceutical and Biomedical Analysis 57: 125- 132.
6. Liu X, Peng Y, Qua X, Ai S, Han R, et al. (2011) Multi-walled carbon nanotube-chitosan/poly(amidoamine)/DNA nanocomposite modified gold electrode for determination of dopamine and uric acid under coexistence of ascorbic acid. Journal of Electroanalytical Chemistry 654: 72-78.
7. Arora K, Sumanaa G, Saxena V, Gupta RK, Gupta SK, et al. (2007) Improved performance of polyaniline-uricase biosensor. Analytica Chimica Acta 594: 17-23.
8. Zen JM, Lai YY, Yang HH, Kumar AS (2002) Multianalyte sensor for the simultaneous determination of hypoxanthine, xanthine and uric acid based on a preanodized nontronite-coated screen-printed electrode. Sensors and Actuators B 84: 237-244.

9. Zhang FF, Li X, Li CX, Li XH, Wan Q, et al. (2005) SnO_2 ref Assay for uric acid level in rat striatum by a reagentless biosensor based on functionalized multi-wall carbon nanotubes with tin oxide. Anal. Bioanal. Chem 382: 1368-1373.

10. Saha S, GuptaV, Sreenivas K, Tan HH, Jagadish C (2010) Third generation biosensing matrix based on Fe-implanted ZnO thin film. Applied Physics Letters 97: 133704.

11. Saha S, Tomar M, Gupta V (2012) Fe doped ZnO thin film for mediator-less biosensing application. J Appl Phys 111: 102804.

12. Liu C, Mensching B, Zeitler M, Volz K, Rauschenbach B (1998) Ion implantation in GaN at liquid-nitrogen temperature: Structural characteristics and amorphization. Physical Review B 57: 2530-2535.

13. Janjua SA, Shah SH, Mehmood A, Zahid F, Mehmood M, et al. (2010) Ion Implantation into Aluminum and Copper by Beam of Carbon Nanoparticles from Regenerative Sooting Discharges. Nucl. Instrum. Methods Phys. Res. B 268: 2785-2789.

14. Li S, Xia J, Liu C, Cao W, Hu J, et al. (2009) Direct electrochemistry of cytochrome c at a novel gold nanoparticles-attached ions implantation-modified indium tin oxide electrode. J Electroanal Chem 633: 273-278.

15. Sharma A, Tomar M, GuptaV (2011) SnO_2 thin film sensor with enhanced response for NO_2 gas at lower temperatures. Sensors and Actuators B 156: 743-752.

16. Saha S, GuptaV (2011) Al and Fe co-doped transparent conducting ZnO thin film for mediator-less biosensing application. AIP Advances 1: 042112.

17. Bentley FF, Smithson LD, Rozek AL (1968) Infrared Spectra and Characteristic Frequencies. Interscience Publishers, New York, London and Sydney.

18. Milligan DE, Jacox ME (1963) Infrared spectroscopic evidence for the species HO_2. J Chem Phys 38: 2627-2632.

19. Nathaly CM, Osvaldo N, Oliveira J, Caseli L (2012) Immbolization of uricase enzyme in Langmuir and Langmuir-Blodgett films of fatty acids: Possible use as a uric acid sensor. J Colloid Interface Sci 373: 69-74.

20. Ali USM, Alvia NH, Ibupoto Z, Nur O, Willander M, et al. (2011) Selective potentiometric determination of uric acid with uricase immobilized on ZnO nanowires. Sensors and Actuators B 152: 241-247.

21. Schrenkhammer P, Wolfbeis OS (2008) Fully reversible optical biosensors for uric acid using oxygen transduction. Biosensors and Bioelectronics 24: 994-999.

22. Miland E, Miranda AJ (1996) Poly(o-aminophenol)-modified bienzyme carbon paste electrode for the detection of uric acid. Talanta 43: 785 796.

23. Chauhan N, Pundir CS (2011) An amperometric uric acid biosensor based on multiwalled carbon nanotube-gold nanoparticle composite. Analytical Biochemistry 413: 97-103.

24. Revin SB, John SA (2012) Selective determination of l-tyrosine in the presence of ascorbic and uric acids at physiological pH using the electropolymerized film of 3-amino-5-mercapto-1,2,4-triazole. Sensors and Actuators B 161: 1059-1066.

25. Arora J, Nandwani S, Bhambi M, Pundir CS (2009) Fabrication of dissolved O_2 metric uric acid biosensor using uricase epoxy resin biocomposite membrane. Analytica Chimica Acta 9: 647,195-201.

26. Luo YC, Doa JS, Liu CC (2006) An amperometric uric acid biosensor based on modified Ir-C electrode. Biosensors and Bioelectronics 22: 482-488.

27. Rawal R, Chawla S, Chauhan N, Dahiya T, Pundir CS (2012) Construction of amperometric uric acid biosensor based on uricase immobilized on PBNPs/cMWCNT/PANI/Au composite. International Journal of Biological Macromolecules 50: 112-118.

28. Behera S, Raj RC (2007) Self-assembled monolayers of thio-substituted nucleobases on gold electrode for the electroanalysis of NADH, ethanol and uric acid. Sensors and Actuators B 128: 31-38.